ORIGINAL RESEARCH

Health Science Reports _Open Access_ WILEY

Unlocking the medicinal arsenal of *Cissus assamica*: GC-MS/MS, FTIR, and molecular docking insights

Mohammad Abdullah Taher[1,2] ⓘ | Ripa Kundu[2,3] | Aysha Akter Laboni[1] | Suriya Akter Shompa[3] | Md. Moniruzzaman[1] | Mohammad Mahmudul Hasan[4] | Hasin Hasnat[3] | Md. Mehedi Hasan[1] | Mala Khan[1]

[1]Bangladesh Reference Institute for Chemical Measurements (BRiCM), Laboratory Road, Dhaka, Bangladesh

[2]Department of Pharmaceutical Chemistry, Faculty of Pharmacy, University of Dhaka, Bangladesh

[3]Department of Pharmacy, State University of Bangladesh, Dhaka, Bangladesh

[4]Department of Chemistry, University of Dhaka, Bangladesh

Correspondence
Mala Khan and Mohammad Abdullah Taher, Bangladesh Reference Institute for Chemical Measurements (BRiCM), Laboratory Rd, Dhaka, 1205, Bangladesh.
Email: dg.mic@bricm.gov.bd and taher.du.pharma@gmail.com

Abstract

Background and aims: This study investigated the biochemical components present in the leaves of *Cissus assamica*. The primary aim was to analyze these components using advanced techniques and assess their potential therapeutic applications.

Methodology: Fourier Transform Infrared (FT-IR) spectroscopy, Gas Chromatography-Mass Spectrometry (GC-MS), and Mass Spectral analysis were employed to identify and characterize the compounds in *Cissus assamica* leaves. The mass spectra of each compound were compared with data from the Wiley and NIST libraries to determine their names, molecular masses, and chemical structures. FT-IR analysis identified characteristic functional groups by their specific frequencies.

Results and discussion: FT-IR spectroscopic analysis revealed significant molecular vibrations at frequencies of 3265.63, 2853.81, 1638.60, 1469.21, and 1384.95 cm^{-1}, indicating the presence of specific functional groups. The GC-MS analysis identified distinct compounds, such as "aR-Turmerone," "Curlone," "7,8-Epoxylanostan-11-ol, 3-acetoxy-," "13-Docosenamide, (Z)-," "Phenol, 3,5-bis(1,1-dimethylethyl)-," "9,19-Cyclolanostan-3-ol, 24,24-epoxymethano-, acetate," and "Quinoline-5,8-dione-6-ol, 7-[[(4-cyclohexylbutyl)amino]methyl]-." These compounds exhibited potential therapeutic applications. Their cytotoxic, antimicrobial, antidiarrheal, anti-hyperglycemic, and pain-relieving properties were evaluated by comparing them with reference ligands targeting specific receptors, including dihydrofolate reductase (DHFR), epidermal growth factor receptor (EGFR), kappa opioid receptor (KOR), glucose transporter 3 (GLUT 3), and cyclooxygenase 2 (COX-2).

Conclusion: The results of this study suggest that Cissus assamica leaves contain bioactive compounds with potential therapeutic benefits for treating infections, diarrhea, hyperglycemia, and pain. However, further research is needed to conduct comprehensive phytochemical screening and establish the precise mechanisms of action for the crude extract or the plant-derived compounds.

KEYWORDS
FT-IR, GC–MS/MS, molecular docking, receptor

1 | INTRODUCTION

New drug candidates have always come from nature, originating from various sources, including plants, minerals, animals, and marine life.[1] Since most novel or current medications found to date are metabolites of plant origin, the plant origin is notably the most important source for treatment from human existence.[2–7] Eighty percent of drug compounds are refined versions of natural plant extract components or direct derivatives of those natural components.[8,9] The extraction of plant materials employs both traditional and innovative techniques. These include maceration, infusion, percolation, digestion, decoction, Soxhlet distillation, turbo-extraction, ultrasound assistance, supercritical fluid extraction, solid-phase extraction, and microwave methods. Modern extraction technologies encompass gas chromatography, chiral phase chromatography, high-performance liquid chromatography, and ionic liquid extraction.[10] Recent focus on organic molecules from plants and their activities has led to increased utilization of GC-MS/MS and LC-MS/MS, chosen based on compound volatility.[11] However, there is a lack of bioactivity evaluation of the isolated compounds.[12] Natural product scientists endeavor to find scientific evidence to support the traditional uses of various medicinal plant species in developing countries, where herbal medicines are most popular.[13] Based on conventional uses, plant crude extracts are usually investigated for certain illness conditions in in-vitro or in-vivo disease models.[14,15] Bioactivity assays are useful but not definitive for traditional usage validation. Despite its limitations, molecular docking is valuable in drug discovery. It screens compounds, saves time, offers unique scaffolds, and uncovers new medicinal plant applications.[16–18]

There are over 350 species in the genus *Cissus*, at least 12 of which are used worldwide in traditional medicine to cure various illnesses.[19] *Cissum assamica* (Lawson) Craib is a species in the Vitaceae family that is locally recognized as Amasha lata and tribally known as Sarba amila or Murmuijja amila. This big, woody climber has angular, reddish-spotted stems; round, cordate or orbicular, cuspidate leaves; tiny, umbellate-opposed axillary leaf cymes of flowers; turbinate, black fruits the size of peas.[20] In the literature survey, few bioactive phytoconstituent of this plant, including 3,3′-dimethyl ellagic acid, disco strain, beta-sitosterol, bergenin, lupeol, n-hexanoic acid, isolariciresinol-9-O-beta-D glucopyranoside, and lupeol, ursolic acid were isolated through preliminary chemical investigations.[21] Fresh *Cissus assamica* stems were used to separate 55 different components, including 11 triterpenes, 9 steroids, 5 tocopherols, 5 chlorophylls, 4 flavonoids, 2 benzoquinones, 2 tannins, and 3 other compounds. Their structures were discovered by correlating their spectrum results with those found in literature publications. They were built using mass spectral data and 1D and 2D nuclear magnetic resonance (NMR) data.[22] However, extensive and further chemical investigations of this plant's parts are necessary for it to be well-established.

It is reported that the methanolic leaf extract of C. assamica possesses significant antipyretic (both central and peripheral) activity.[20] Scholars have identified betulinic acid and *epi*-glut-5(6)-en-ol

Highlights

- Compound isolation and characterization of the plant *Cissus assamica* was done by GC-MS/MS and FTIR analyses.
- A total of 15 Phytochemicals were identified.
- In silico analysis of the identified phytochemicals were carried out for the evaluation of antidiarrheal, analgesic, hypoglycemic, anticancer and antimicrobial potentiality of the compounds.
- ADME/T were shown to observe potential drug likeliness.

from C. assamica as having significant cytotoxic effects on the human cell line, suggesting the plant's anticancer properties.[22] In China, this plant is an endothelin antagonist popularly known as an anti-snake venom medicinal herb.[23] C. araloides is proven to have antimicrobial potentials caused by multiresistant infection.[24] One study described the antidiabetic, diuretic, anti-inflammatory, and anticonvulsant properties of the plant C. sicyoides.[25]

Earlier studies utilized NMR techniques (^{1}H, ^{13}C, or 2D NMR) for substance separation from plants. In contrast, we adopted solvent-solvent extraction to isolate bioactive compounds. These compounds were then analyzed using FTIR and GC-MS/MS methods to determine their functional groups and chemical structure. Utilizing NIST 2020 software, we identified targeted compounds by analyzing their fragmented mass and molecular base peak. Furthermore, we assessed the binding affinities of our isolated molecules to five receptors (kappa opioid receptor, GLUT 3, cyclooxygenase 2, DHFR, and EGFR) and evaluated their ADME/T properties.

2 | METHOD

2.1 | Collection of plant

The leaves of the plant *Cissus assamica* (Figure 1) were collected in February 2022 from Jahangirnagar University, which is 32 kilometers from the west side of the Asian highway, sometimes referred to as

FIGURE 1 Leaves of Cissus assamica.

the Dhaka-Aricha Road. The plant was taxonomically recognized and stored for future use as a voucher specimen at the National Herbarium of Bangladesh located in Mirpur, Dhaka.

2.2 | Extraction and partitioning of the crude

After being exposed to the sun for several days, dried leaves were processed and ground into a coarse powder at the State University of Bangladesh's Phytochemistry Research Lab using a high-capacity grinding machine. After grinding the leaves into a powder, 3 L of pure methanol (MeOH) were added to a 5 L brown reagent jar. The jar was sealed and stored for 25 days to allow thorough mixing, occasionally shaken or stirred. Subsequently, the mixture was filtered once using Whatman No. 1 filter paper and a new cotton plug. The filtrate was then dried under vacuum using a rotary evaporator at less than 40°C, yielding approximately 85.5 g of gummy mass. The method developed[26] and modified[27] was used to fractionate the concentrated methanol extract. In brief, 5 g of crude extract was dissolved in 90% methanol and water. The resulting solution was partitioned using polar and non-polar solvents including petroleum ether (C_6H_{14}), chloroform ($CHCl_3$), and ethyl acetate (EtOAc). Organic fractions were dried using a low-temperature rotary evaporator for further analysis, focusing on the plant's crude methanol fractions.

2.3 | GC-MS/MS system condition

Gas Chromatographic techniques (GC-MS/MS) were used to examine the bioactive chemicals that were extracted from the leaves of C. fistula where a well-established method electron impact ionization (EI) method was used connected to a mass detector made by Shimadzu in Kyoto, Japan, and the model name is GC-MS TQ 8040. The column oven temperature was fixed at 50°C. A capillary column fused with silica with the following specifications (Rxi-5 ms, 30 m, 0.25 mm ID, and 0.25 m) was utilized. By keeping the injection temperature constant at 250°C. The sample injection method was in split mode. Preheating was performed in the oven. Preheating the oven was 1 min at 500°C, 2 min at 200°C, and 7 min at 300°C. The compound name, structures, and molecular weights of each extract's bioactive ingredients were determined by comparing its mass spectra with the data found in the NIST and Wiley libraries. Kim et al.,.[18,28,29] It took a total of 39 min to complete the GC-MS run.

2.4 | FTIR analysis

To identify different chemical connections and functional groups present in compounds, one of the most useful instruments is the Fourier transform infrared spectrophotometer c This has made it essential for structural and spectrochemical analytical examinations of a wide range of materials, from tiny molecules[30–32] to more complex materials, macromolecules, and supramolecular structures[33,34] both theoretical and experimental. For the FTIR study, the plant extract was powdered and dried. Setting the FTIR operation in an environment free of dampness is

advised. To prepare a translucent sample disc, 100 mg of KBr pellet and approximately 10 mg of nonaqueous plant crude samples were mixed according to a predetermined protocol. A FTIR imaging instrument of Shimadzu made in Japan featuring a wavelength range of 400 to 4000 cm^{-1} and a spatial resolution of 4 cm^{-1} was used to evaluate the powdered sample from the plant specimen.

2.5 | Molecular docking study

A method based on computing was used to evaluate the binding affinities of compounds isolated from the methanolic leaves extract of Cissus assamica against various target proteins. Several software applications, such as PyMoL 2.3, PyRx, DiscoveryStudio 4.5, and Swiss PDB viewer, were utilized to conduct the analysis.[35]

2.6 | Ligand preparation

PubChem (https://pubchem.ncbi.nlm.nih.gov/) was searched for, and the 3D SDF structures of the chemicals indicated in Table 1 were retrieved (accessed on September 28, 2023). Additionally, 3D SDF structures of five standard compounds, namely Lapatinib (PubChem CID_208908), Ciprofloxacin (PubChem CID_2764), Glibenclamide (PubChem CID_3488), Loperamide (PubChem CID_3955), and Diclofenac (PubChem CID_3033), were obtained from the website sources.[36,38,39,41] A ligand library was generated by systematically importing both the compounds and the standards into Discovery Studio 4.5. Subsequently, plant derived compounds underwent optimization using a semiempirical method featured as Pm6, thereby enhancing the accuracy and precision of the docking process.[37,42]

2.7 | Target protein selection

Fifteen compounds isolated from the methanol fractions of Cissus assamica leaf extract were subjected to computerized docking analysis to explore their potential cytotoxic, antimicrobial, hypoglycemic, antidiarrheal, and analgesic properties. To assess cytotoxicity, the three Dimensional crystal composition of the cytotoxic receptor epidermal growth factor receptor (EGFR) [PDB ID: 1XKK],[36,37] which was taken from the source Protein Data Bank (https://www.rcsb.org/ (accessed on 28 September 2023)). Similarly, the 3D structures of dihydrofolate reductase (DHFR) [PDB ID: 4M6J], (GLUT3) [PDB ID: 4ZWB], (KOR) [PDB ID: 6VI4], and (COX-2) [PDB ID: 1CX2] were downloaded from the same source to evaluate their antimicrobial, hypoglycemic, antidiarrheal, and analgesic activities, respectively.[36,38,39,41]

2.8 | Ligand-protein binding

The affinities and potential binding patterns of phytocompounds with target molecules were assessed using a computer-aided ligand-

TABLE 1 Selection of target site and grid mapping of target receptors.

Receptor	Standard	Target binding sites	Reference	Grid box	
EGFR	Lapatinib	Thr 790, Gln 791, Leu 792, Met 793, Gly 796, Cys 797, Leu 799, Asp 800, Arg 803, Leu 844, Thr 854, Asp 855, Phe 856, Leu 718, Val 726, Ala 743, Lys 745, Met 766, Lys 775, Arg 776, Leu 777, Leu 788	El Azab et al.,[36,37]	Center	$x = 15.9205909709$, $y = 34.3392875093$, $z = 35.6483134052$
				Dimension	$x = 24.8023896568$, $y = 20.1364349659$, $z = 32.7376593496$
DHFR	Ciprofloxacin	Ala9, Ile16, Leu93, Ser92, Arg91, Arg77, Glu78, Ser76, Leu75, Lys54, Val120, Ser119, Lys55, Thr56, Ser118, Gly117, and for 1R4U, Arg 176, Val 227, Gln 228, Asn254, His 256	Khatun et al.,[37,38]	Center	$x = 3.25328265364$, $y = -3.44333744641$, $z = -18.638584512$
				Dimension	$x = 20.4986942064$, $y = 27.8290754574$, $z = 27.0611347059$
GLUT-3	Glibenclamide	PRO194, GLN198, ILE309, GLY312, VAL313, THR347, TRP410, LEU418, PHE442, TYR26, THR28, GLY29, VAL30	Mojica et al.,[39]	Center	$x = 106.593467458$, $y = 10.9952523796$, $z = 60.5261656512$
				Dimension	$x = 45.3478961482$, $y = 23.9394611591$, $z = 33.5106393742$
KOR	Loperamide	Ser 136, Ile 137, Leu 103, Leu 107, Trp 183, Leu 184, Ser 187, Ile 191, Leu 192, Ile 194, Val 195	Alam et al.[40]	Center	$x = 54.2610778594$, $y = -50.3947461549$, $z = -16.1667067677$
				Dimension	$x = 14.963572328$, $y = 28.0308712165$, $z = 17.9591142778$
COX-2	Diclofenac	Ala 516, Phe 518, Val 523, Ala 527, Ser 530, His 90, Gln 192, Val 349, Leu 352, Ser 353, Tyr 355, Tyr 385	Muhammad et al.,[41]	Center	$x = 23.2282573687$, $y = 21.0863728091$, $z = 15.4956082852$
				Dimension	$x = 21.2564348845$, $y = 18.3985967401$, $z = 23.7976510895$

TABLE 2   Predicted Bioactive Compounds from GC-MS/MS.

S/N	R.T	Area %	Chemical Compound	m/z	MS Similarity %
1	3.7	5.54	3,3-Dimethoxy-2-butanone	89	78
2	3.8	2.27	1,3-Dioxolane-4-methanol, 2-ethyl-	103	69
3	10.7	1.74	Phenol, 3,5-bis(1,1-dimethylethyl)-	191	70
4	12.3	36.9	aR-Turmerone	83	92
5	12.8	9.57	Curlone	120	90
6	22.7	25.62	13-Docosenamide, (Z)-	59	86
7	22.8	3.72	Quinoline-5,8-dione-6-ol, 7-[[(4-cyclohexylbutyl) amino] methyl]-	97	62
8	23.2	2.17	1-Decanol, 2-hexyl-	57	77
9	23.7	2.1	2-Methylpiperidine-1-thiocarboxylic acid 2-[1-[2-thiazolyl]ethylidene]hydrazide	57	60
10	24.1	1.63	(E)−3,7,11-Trimethyldodec-2-enoic acid, methyl ester	85	57
11	24.8	1.71	Triacontane, 1,30-dibromo-	85	62
12	25.1	1.82	7,8-Epoxylanostan-11-ol, 3-acetoxy-	85	65
13	29.1	1.52	9,19-Cyclolanostan-3-ol, 24,24-epoxymethano-, acetate	57	52
14	29.4	2.19	Undec-10-ynoic acid, tetradecyl ester	57	60
15	33.0	1.44	tert-Butyl (2-aminophenyl)carbamate, 2TMS derivative	73	50
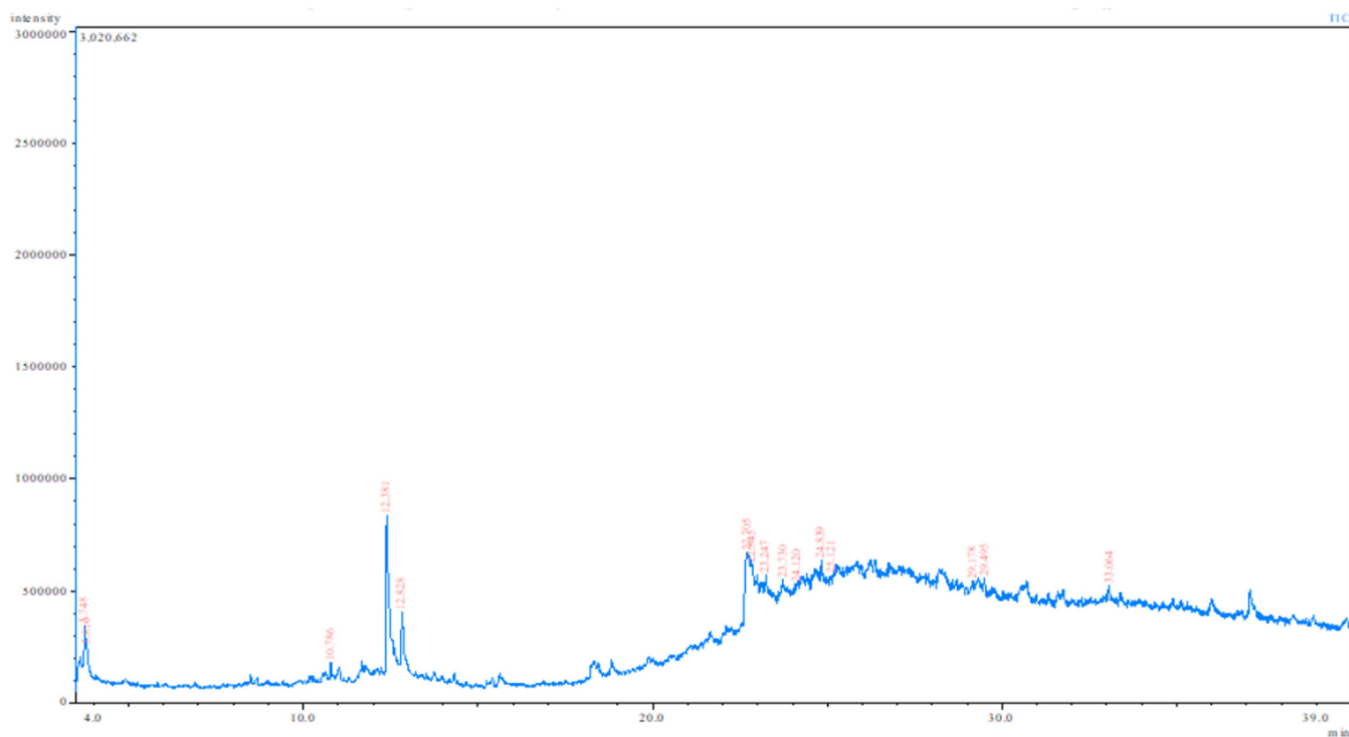
FIGURE 2   GC-MS/MS Chromatogram of the plant C. assamica.

protein interaction diagram. Advanced software, PyRxAutodock Vina, was employed for this drug receptor interaction, utilizing semi-flexible modeling for the docking process. A literature-based selection of specific amino acids with their IDs was made for individual receptors to ensure precise target docking. The protein was prepared by loading and formatting it as the necessary macromolecule, ensuring ligands exclusively bind to the intended target.

Open Babel in PyRxAutoDock Vina software was used to import the ligands' SD files and convert them into the pdbqt format for obtaining the best possible docking in respect to these designated structures. Active amino sites were defined within grid boxes using grid mapping, with the center and dimension axes specified in Table 1 being maintained during the docking process. Default supportive functions were retained at this stage. Subsequently, Employing AutoDock Vina (version 1.1.2), a final docking study was performed to ascertain the ligands' affinity for the corresponding macromolecule. The final step involved interpreting the results and employing BIOVIA Discovery Studio version 4.5 to predict the most suitable 2D and 3D models.

2.9 | ADME/T analysis

In computer-based molecular drug design, pharmacokinetic studies are increasingly popular. These encompass absorption, distribution, metabolism, excretion, and toxicity analysis. Bioavailability and drug-likeness determination, along with ADMET analyses, play key roles in drug discovery, accessible through resources like http://biosig. unimelb.edu.au/pkcsm/prediction. Online platforms like Swis-sADME (http://www.sib.swiss) are widely employed to predict drug likeness based on Lipinski rules and pharmacokinetic parameters. According to Lipinski, a compound is considered orally accessible if it meets specific criteria, including a molecular weight below 500 amu
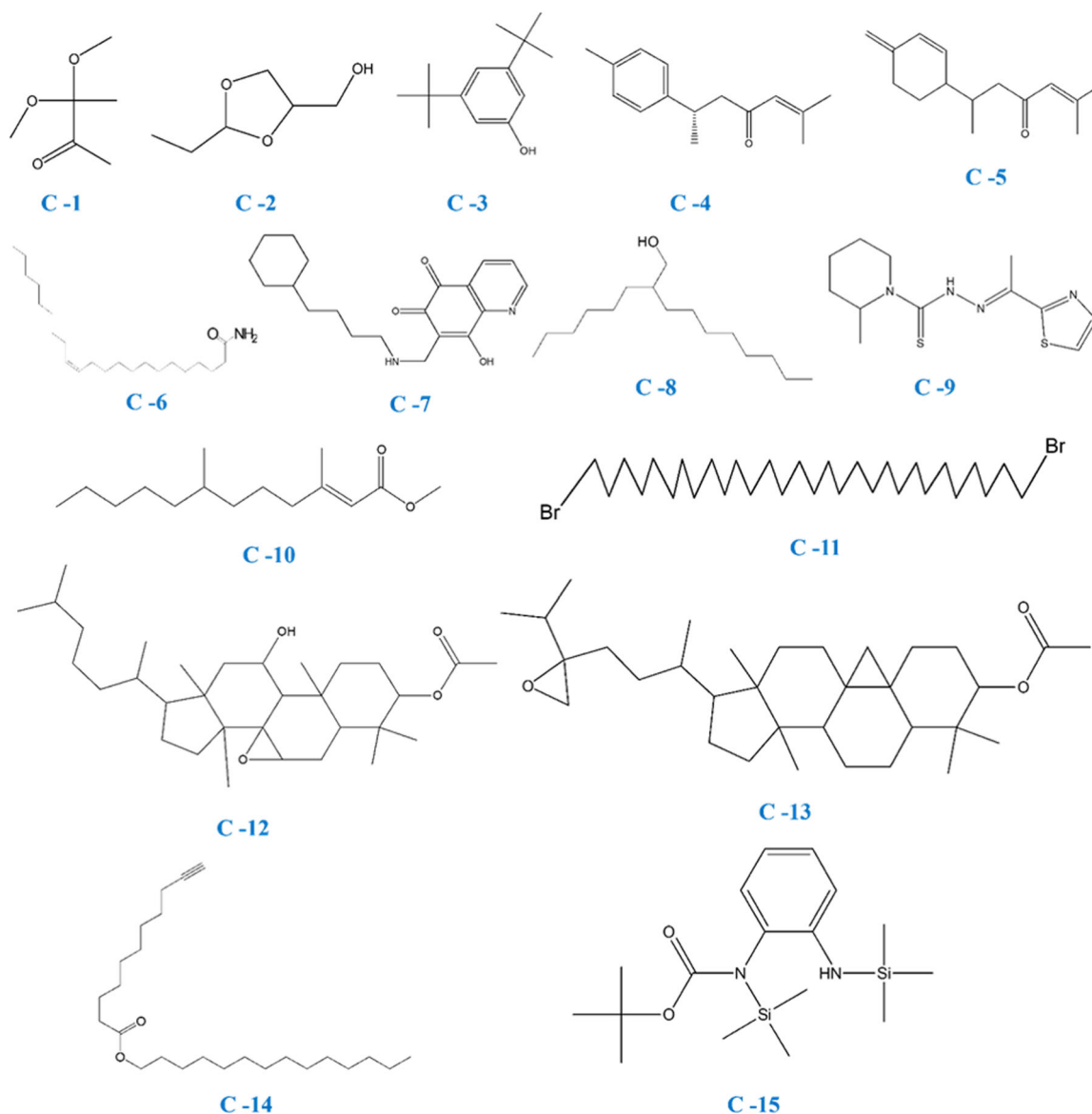

FIGURE 3 Structure of the identified compounds from C. assamica.

and a lipophilicity value (LogP) of ≤5. In addition, hydrogen bond donor sites will be below five to fulfil the criteria, and hydrogen bond acceptor sites will be less than.[37,43]

3 | RESULT

3.1 | Prediction of compounds by GC-MS/MS

Through investigating the samples' chemical constitution and structure, different medicinal plant extracts can be found to have a wide range of biological potential. To the best of our knowledge, however,

no research on GC-MS/MS-based characterization has been published to identify different bioactive chemicals present in methanolic extracts of the *C. assamica* plant. As a result, the GC–MS/MS evaluation was performed in a planned investigation. This plant fraction showed a total of 15 peaks, each identifying a bioactive molecule that was recorded by comparing its molecular mass, chemical formula, and peak retention time to those of the compounds the NIST library identified as recognized.

To show the relative concentration of each component, we measured the peak area percent. The most abundant bioactive compounds are aR-Turmerone (36.9%), 13-Docosenamide, (Z)- (25.6%), Curlone (9.57%), 3,3-Dimethoxy-2-butanone (5.54%), Quinoline-5,8-dione-6-ol,

TABLE 3 FT-IR fingerprint studies and functional groups of the extract of C. assamica.

| Absorption (Cm^{-1})	Peak Intensity	Characteristics Group	Assumed phyto-compounds
3265.63	medium	O-H str. Hydroxyl	Glycosides, Tannins, Flavonoids, Saponins
2924.21	medium	C-H stretching	Alkane
2853.81	Weak	CH$_2$ str.	Aliphatic compounds, Steroids, Saponins, flavonoids
1638.60	strong	C = O stretching	Steroidal glycosides, Flavonoids, alkene
1619.31	medium	C = C stretching	
1469.21	medium	CH$_2$ bend (Alkane, Asymmetrical)	Aliphatic compounds, Steroids, Saponins, flavonoids
1384.95	sharp		Steroidal glycosides, Flavonoids, Saponins, hexose sugars
1126.48	sharp	C-C-C bend	Flavonoid
616.28	sharp	S-S bond	Glycosides
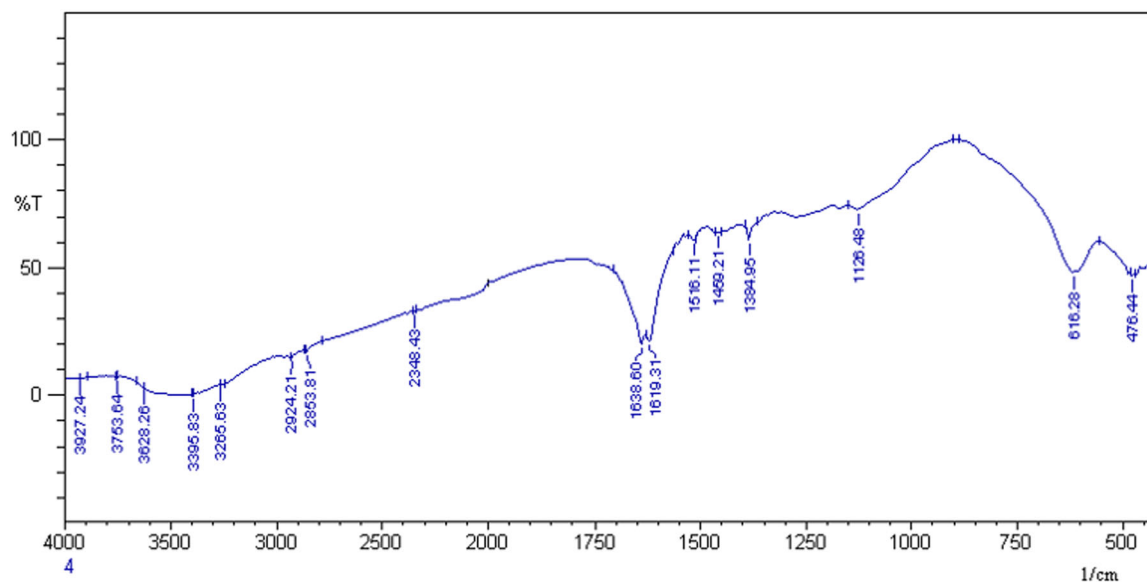
FIGURE 4 FTIR spectrum of the plant extract.

7-[[(4-cyclohexylbutyl)amino]methyl]- (3.72%), and Phenol, 3,5-bis(1,1-dimethylethyl)- (1.74%). The retention time of each compound has been placed in Table 2 and Figure 2. By analyzing the data in Table 2, it is evident that the mass spectrum of the compound closely aligns with known spectra, resulting in the identification of the specific structure shown in Figure 3.

3.2 | FTIR analysis for determining functional group

In accordance with the absorbance range of the infrared radiation spectrum, characteristics of the compounds nature was revealed. Based on the peak ratio, the structural categories of the constituents were divided following the FTIR processing of the extract. The existence of the functional groups $C = O$, $C = C$, $S-S$, $O-H$ bonds, and $C-H$ was assured which is shown in Table 3. It has been proven that

FTIR spectroscopy is an appropriate and sensitive method for figuring out what kinds of molecules are in them.

Numerous peaks at different fingerprint areas were detected by FT-IR spectroscopy (Figure 4), showing the existence of many functional groups, including tannins, steroids, glycosides, flavonoids, and sesquiterpenes. The most prevalent substances were sesquiterpenes and steroids (Table 3). The confirmation of phenolic or polyphenolic compounds such as steroids, flavonoids, tannins, glycosides, and saponins is suggested by the existence of phenolic O-H group, which is represented at $3265.63\,cm^{-1}$. Additional prominent intensity peaks detected at 1126.48 and $616.28\,cm^{-1}$ suggested the existence of flavonoids and glycosides. Flavonoids, steroids, saponins, and hydrocarbon compounds were detected by the absorbance at $2853.32\,cm^{-1}$ with CH_2 elongation. Thus, the existence of the phenolic group, glycosides, steroids, flavonoids, and saponins was demonstrated by the FT-IR spectral analysis.[44,45]

TABLE 4 Docking score (kcal/mol) of identified compounds from methanol extract of leaves of C. assamica.

|		Targets				
Serial	Compounds	EGFR	DHFR	GLUT-3	KOR	COX-2
C1	3,3-Dimethoxy-2-butanone	−4.7	−4.1	−4.7	−4	−4.5
C2	1,3-Dioxolane-4-methanol, 2-ethyl-	−5.1	−4.6	−5.1	−4.3	−5.1
C3	Phenol, 3,5-bis(1,1-dimethylethyl)-	−7	−6.3	−7.6	−7.1	−6.6
C4	aR-Turmerone	−7.5	−6.4	−7.3	−7.4	−7.9
C5	Curlone	−7.5	−6.5	−7.7	−7.5	−8.1
C6	13-Docosenamide, (Z)-	−6.6	−5.3	−6.7	−6.2	−7.3
C7	Quinoline-5,8-dione-6-ol, 7-[[(4-cyclohexylbutyl)amino]methyl]-	−8.9	−7.9	−9.1	−8.7	−8
C8	1-Decanol, 2-hexyl-	−6.5	−5.1	−6.3	−5.8	−6.3
C9	2-Methylpiperidine-1-thiocarboxylic acid 2-[1-[2-thiazolyl]ethylidene]hydrazide	−7.2	−6.5	−7.2	−6.6	−7.3
C10	(E)−3,7,11-Trimethyldodec-2-enoic acid, methyl ester	−7	−5.6	−6.8	−6.6	−7.2
C11	Triacontane, 1,30-dibromo-	−5.5	−5.1	−6.6	−5.9	−6.5
C12	7,8-Epoxylanostan-11-ol, 3-acetoxy-	−9	−7.3	−7.9	−8.1	1.6
C13	9,19-Cyclolanostan-3-ol, 24,24-epoxymethano-, acetate	−8.5	−7.8	−8.5	−9.8	−5.3
C14	Undec-10-ynoic acid, tetradecyl ester	−6.3	−5.6	−6.2	−5.6	−4.7
C15	tert-Butyl (2-aminophenyl)carbamate, 2TMS derivative	−1.1	−0.9	−1.2	−0.9	−1
Standard	Lapatinib	−10.9	-	-	-	-
	Ciprofloxacin	-	−8.1	-	-	-
	Glibenclamide	-	-	−10.2	-	-
	Loperamide	-	-	-	−9.3	-
	Diclofenac	-	-	-	-	−7.8
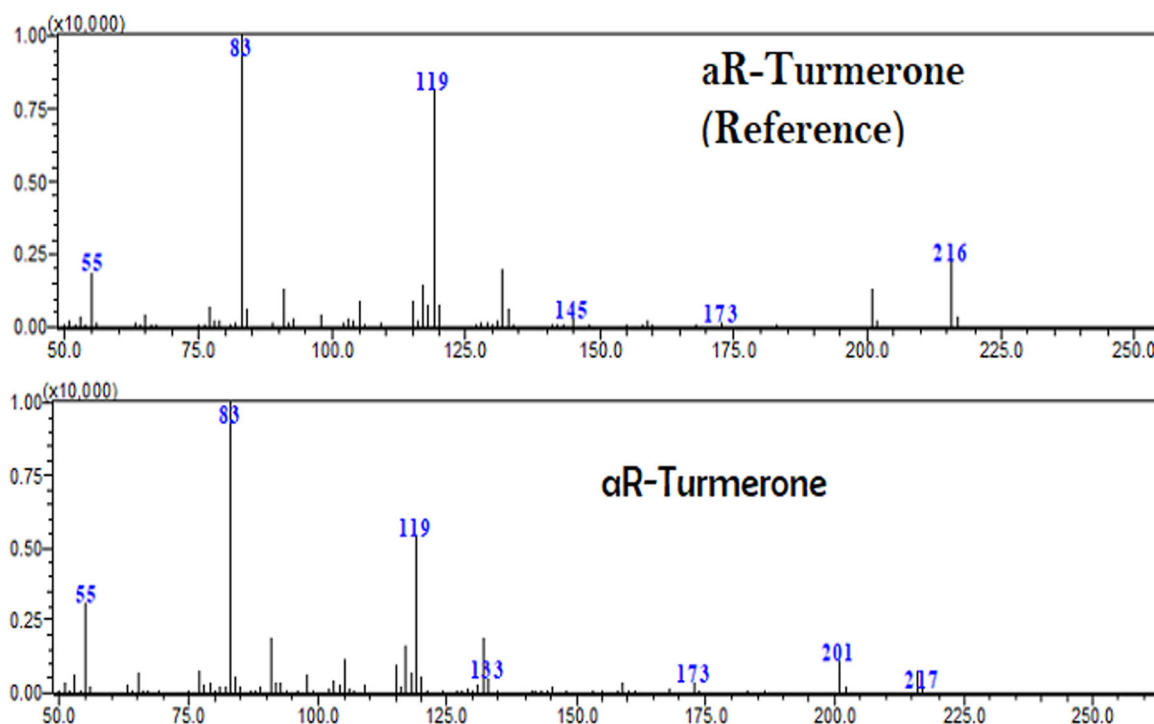
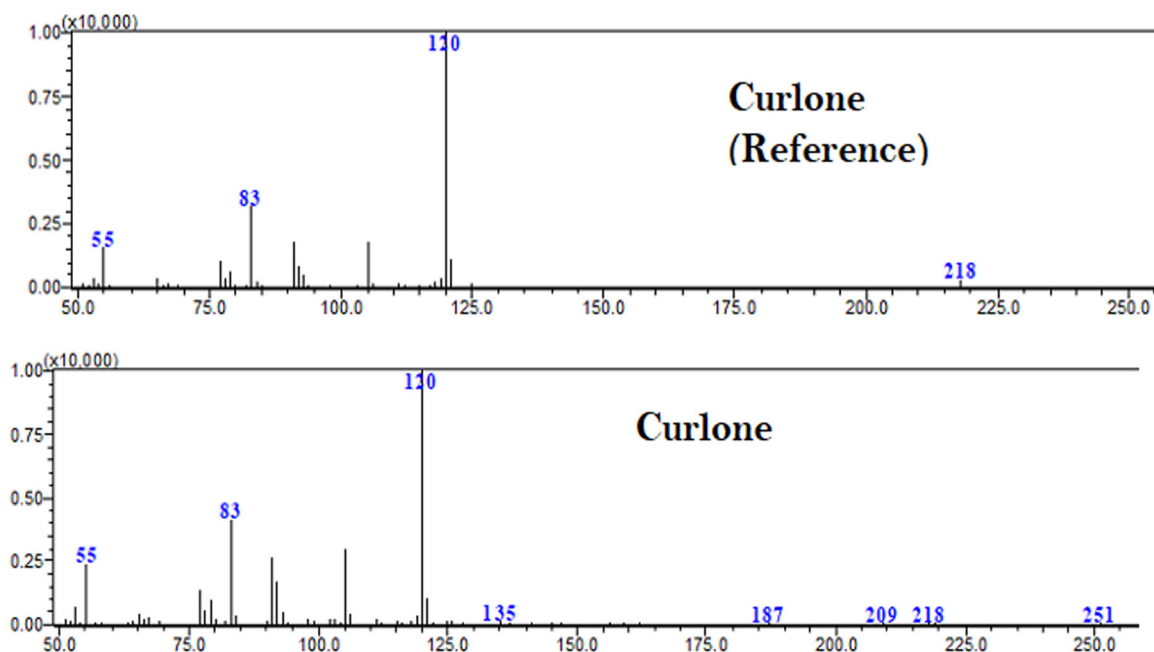**FIGURE 5**   m/z value of aR-Turmerone with reference by GC-MS/MS.

FIGURE 6   m/z value of Curlone with reference by GC-MS/MS.

3.3 | Molecular docking result

The 15 identified compounds from methanol extract of leaves of *Cissus assamica* has been gone through computational docking studies against five different receptors. Table 4 represented binding affinities of these compounds towards the receptors. For target EGFR, the C12 exhibited prominent binding affinity with a values of −9 kcal/mol followed by C7 (−8.9 kcal/mol) and C13 (−8.5) compared to standard lapatinib which showed a value of −10.9 kcal/mol. However, C4 and C5 were manifested promising affinity against the receptor with value of −7.5 kcal/mol. In comparison to standard ciprofloxacin's binding value −8.1 kcal/mol, the compound 7 and 13
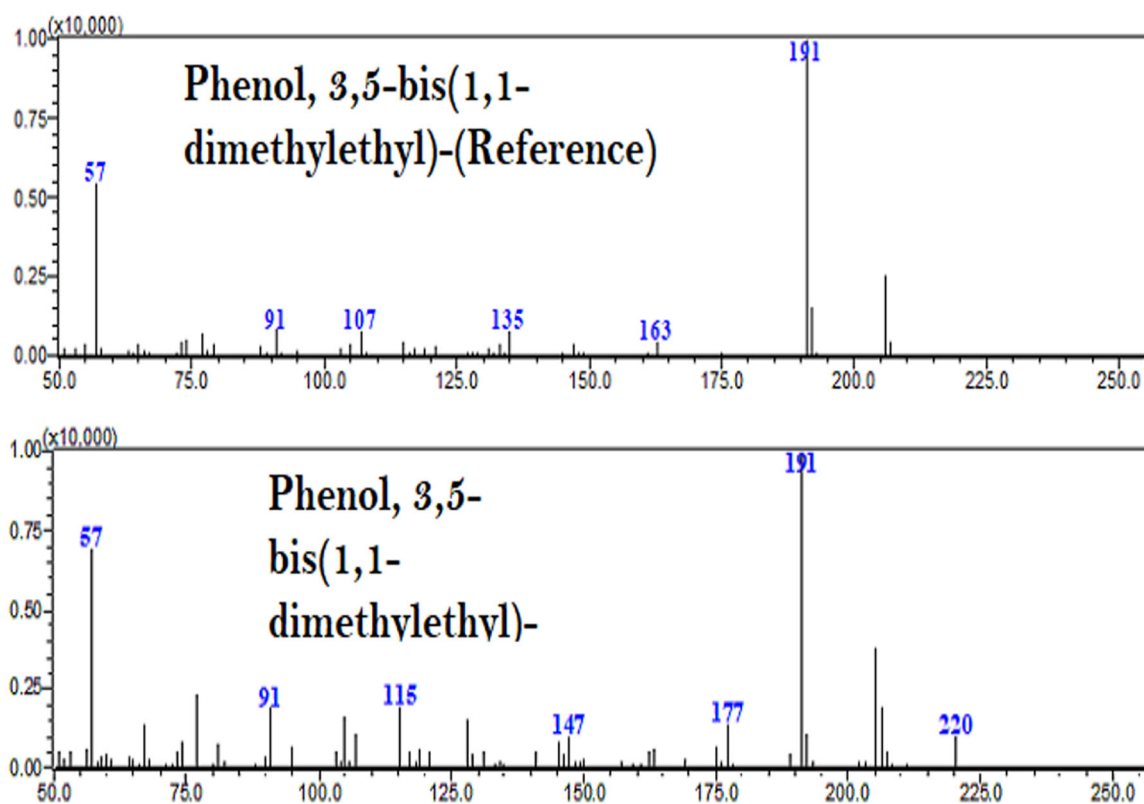
FIGURE 7 m/z value of Phenol, 3, 5-bis(1,1- dimethylethyl) with reference by GC-MS/MS.

exhibited very promising affinities towards DHFR with values of −7.9 and −7.8 kcal/mol respectively. Additionally, compound 3, 4, 5, and 9 showed lower value than −6 kcal/mol The highest binding against GLUT-3 was observed for C7 with a value of −9.1 kcal/mol which almost reach the value of standard glibenclamide (−10.2 kcal/mol). Khatun et al.,.[37,38]

In addition, C13 scored −8.5 kcal/mol, where C3, C4, and C5 illustrated lower affinities than −7 kcal/mol. Surprisingly, C13 exhibited very prominent activity towards KOR with a value of −9.8 kcal/mol which suppressed the standard lipoamide score −9.3 kcal/mol. Moreover, C7 and C12 scored −8.7 and −9.1 kcal/mol respectively. In the case of COX-2 most of the compounds illustrated promising binding affinities, specially C5 and C8 showed affinities value of −8.1 and −8 kcal/mol respectively which suppressed standard diclofenac docking score −7.8 kcal/mol.

4 | DISCUSSION

4.1 | Characterization and pharmacology of compounds

Despite having similar chemical structures, ar-turmerone, turmerone, and curlone can be easily identified from one another using split ions peaks in mass spectrometry (GC-MS/MS). Benzene and methylheptenone are present in ar-turmerone., which can be de-electronized to generate $C_{15}H_{20}O + (m/z = 216)$, as can be seen in Figure 5 of the mass spectrum. $C_{14}H_{17}O +$ is produced by demethylation (-CH_3) ($m/z = 201$). Higher abundances of $C_5H_7O + (m/z = 83)$ and $C_9H_{11} + (m/z = 119)$ result from further cleavage. This is due to the ease with which aromatic compounds can delocalize to stabilize a positive charge.[46]

Whereas, A cyclohexadiene and a methylheptenone combine to form turmerone. After demethylating (-CH_3) to produce $C_{14}H_{19}O +$ ($m/z = 203$), turmerone underwent further cleavage to produce the more abundant form $C_5H_7O + (m/z = 83)$. Ar-turmerone has been shown in multiple instances to possess cytotoxic and analgesic properties.[47,48] In particular, ar-turmerone inhibits the inflammatory activation of cultured microglia caused by LPS or β-amyloid.[49] Additionally, it prevents glial activation and memory impairment brought on by intraperitoneal and chronic LPS administration[50,51] and promotes neural stem cell proliferation and neuronal differentiation. When combined, ar-turmerone may shield dopaminergic neurons in Parkinson's disease models from the inflammatory toxicity of activated microglia.

As a sesquiterpene chemical, curlone is classified in Figure 6. $C_{14}H_{17}O + (m/z = 201)$ was produced during dehydrogenation (-H) and demethylation (-CH_3), and it subsequently broke down to produce $C_9H_{12} + (m/z = 120)$ in high abundance.[46] Curlone derived from Curcuma oil has been reported to scavenge free radicals, which indicates its antioxidant properties and exerts significant anti-inflammatory as well as antinociceptive activities.[52,53] Antidiabetic properties of the compound is well
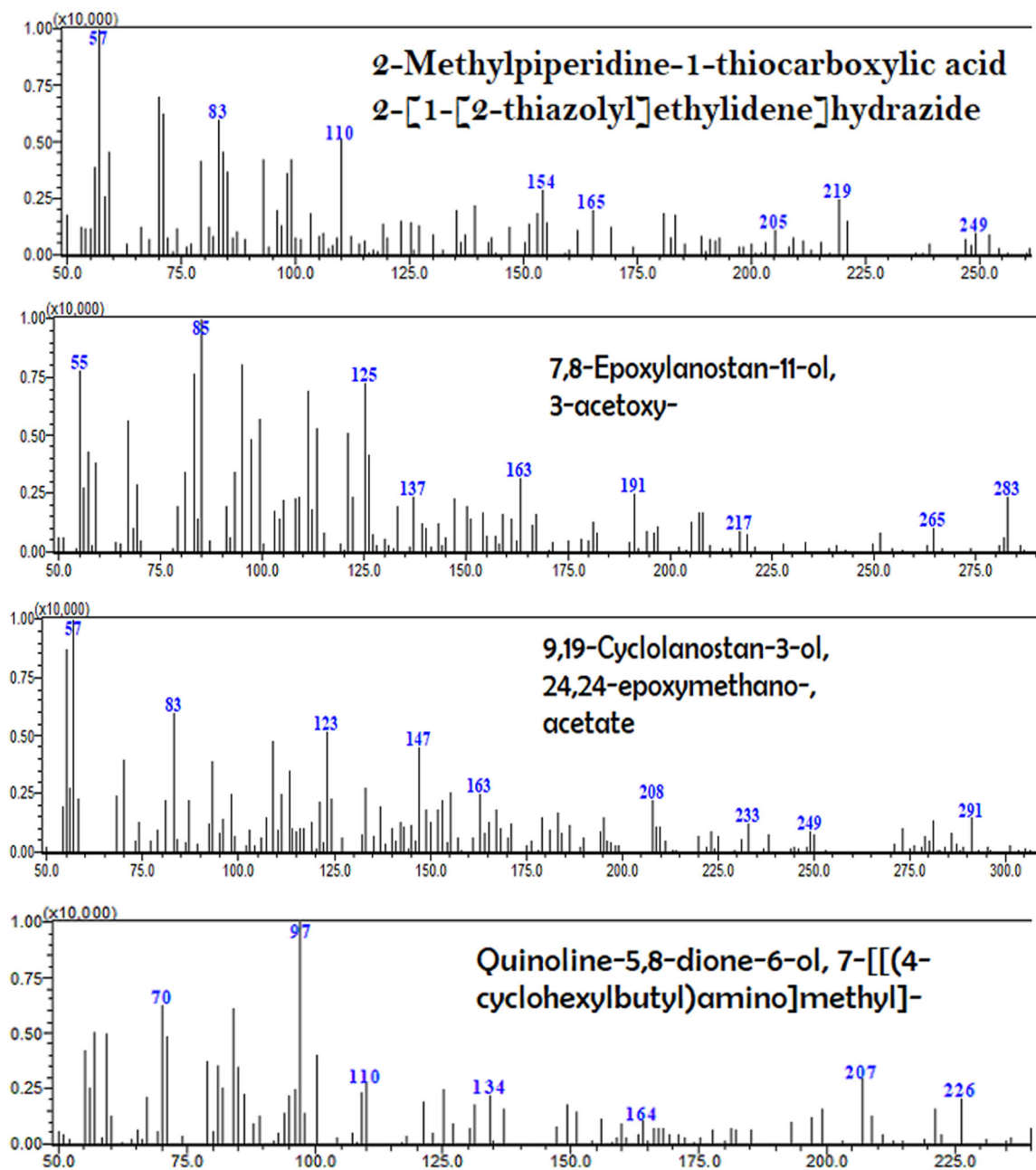
FIGURE 8   m/z value of 2-Methylpiperidine-1-thiocarboxylic acid 2-[1-[2-thiazolyl]ethylidene]hydrazide, Quinoline-5,8-dione-6-ol, 7-[[(4-cyclohexylbutyl)amino]methyl]-, 9,19-Cyclolanostan-3-ol, 24,24-epoxymethano-, acetate, 7,8-Epoxylanostan-11-ol, 3-acetoxy- in GC-MS/MS.

reported by the scientist. In hamsters and rats, Curcuma oil reduces insulin resistance and related thrombotic problems.[54] The plant's cardiovascular activity was evaluated where Curcuma oil-derived compounds (Curlone, ar-turmerone) appear to be a safe and effective antiplatelet therapy that prevents vascular clotting by promoting blood circulation.[55] Scholars have reported the antibacterial potentiality of the compounds.[56] Another study showed that compounds derived from Curcuma oil attenuate nitrosative and oxidative stress, considerably reducing ischemia's negative effects.[57] To ensure the safety of the compounds, a genotoxicity and mutagenicity study was performed.[58]

In Figure 7, Phenol, 3,5-bis(1,1-dimethyl ethyl)- is 70% similar to the mass spectrometry data of the reference. In the mass spectrum, the highest abundance of m/z of 191 produced fragments m/z of 57 and 91. By increasing insulin secretion and blood insulin levels, insulin secretagogues lower blood glucose and help control diabetes. Over the past three decades, plenty of investigations have been carried out to create an insulin-secreting beta cell line that retains normal control over insulin secretion, but very few these have been successful.[59] In this work, isolated mouse pancreatic islets were stimulated to produce insulin in a concentration-dependent manner by nontoxic doses of phenol, 3,5-bis(1,1-dimethylethyl).[60]

TABLE 5 Bond and binding site of two highly active two compounds against different targets including EGFR, DGFR, GLUT-3, KOL, and COX-2.

| Receptor	Compounds	Binding affinities (kcal/mol)	Bond type	Amino acids
EGFR	C7	−8.9	Alkyl	Leu 718, Val 726, Ala 743, Lys 745, Cys 797, Leu 844
			Carbon-hydrogen	Arg 841
	C12	−9	Alkyl	Leu 718, Val 726, Ala 743, Lys 745, Met 766, Leu 777, Leu 788, Leu 844, phe 856
			Carbon-hydrogen	Asp 855
	Lapatinib	−10.9	Alkyl	Leu 718, Val 726, Ala 743, Met 766, Cys 775, Leu 777, Leu 844
			Hydrogen	Lys 745, Phe 856
			Unfavorabol donor	Met 793
			Carbon-hydrogen	Ser 720, Gly 721, Gln 791
DGFR	C7	−7.9	Alkyl	Leu 22, Phe 34
			Hydrogen	Ala 9, Ile 16, Val 115, Tyr 121
	C13	−7.8	Alkyl	Val 8, Ile 16, Leu 22, Lys 55, Tyr 121
			Hydrogen	Ala 9
	Ciprofloxacin	−8.1	Alkyl	Ile 16, Leu 22
			Hydrogen	Ala 9, Glu 30, Ser 118
			Carbon-hydrogen	Tyr 121
GLUT-3	C7	−9.1	Alkyl	Val 67, Phe 70, Ile 166, Ile 285, Phe 289, Phe 377
			Pi-sigma	Thr 28
	C13	−8.5	Alkyl	Ile 19, Phe 22, Leu 157, Leu 160, Val 164, Phe 190, Pro 194, Leu 197
	Glibenclamide	−10.2	Alkyl	Ala 68, Ile 285, Tyr 290, Phe 414, Gly 417, Leu 418
			Hydrogen	Asn 32, Val 67, Asn 286
KOR	C7	−8.7	Alkyl	Tyr 140, Trp 183, Ile 191, Val 195
			Carbon-hydrogen	Ile 180
	C13	−9.8	Alkyl	Leu 103, Ile 137, tyr 140, Ile 180, Leu 184, Ile 191
			Pi-sigma	Trp 183
	Loperamide	−9.3	Alkyl	Ile 180, Val 195
			Pi-sigma	Trp 183, Leu 184, Ile 191
			Pi-donor H-donor	Ser 136
			Pi-Pi	Tyr 140
COX-2	C5	−8.1	Alkyl	Val 116, Val 349, Leu 352, Leu 359, Tyr 385, Trp 387, Val 523, Leu 531, Leu 359
			Hydrogen	Arg 120, Tyr 355
	C7	−8	Alkyl	Val 349, Leu 352, Tyr 355, Leu 384, Tyr 385, Trp 387, Val 523, Ala 527,
			Hydrogen	Ser 530
			Carbon-Hydrogen	Met 522
			Amide-pi	Gly 526
	Diclofenac	−7.8	Alkyl	Leu 352, Gly 526, Leu 531
			Hydrogen	Tyr 355
			Pi-sigma	Val 349, Ala 527
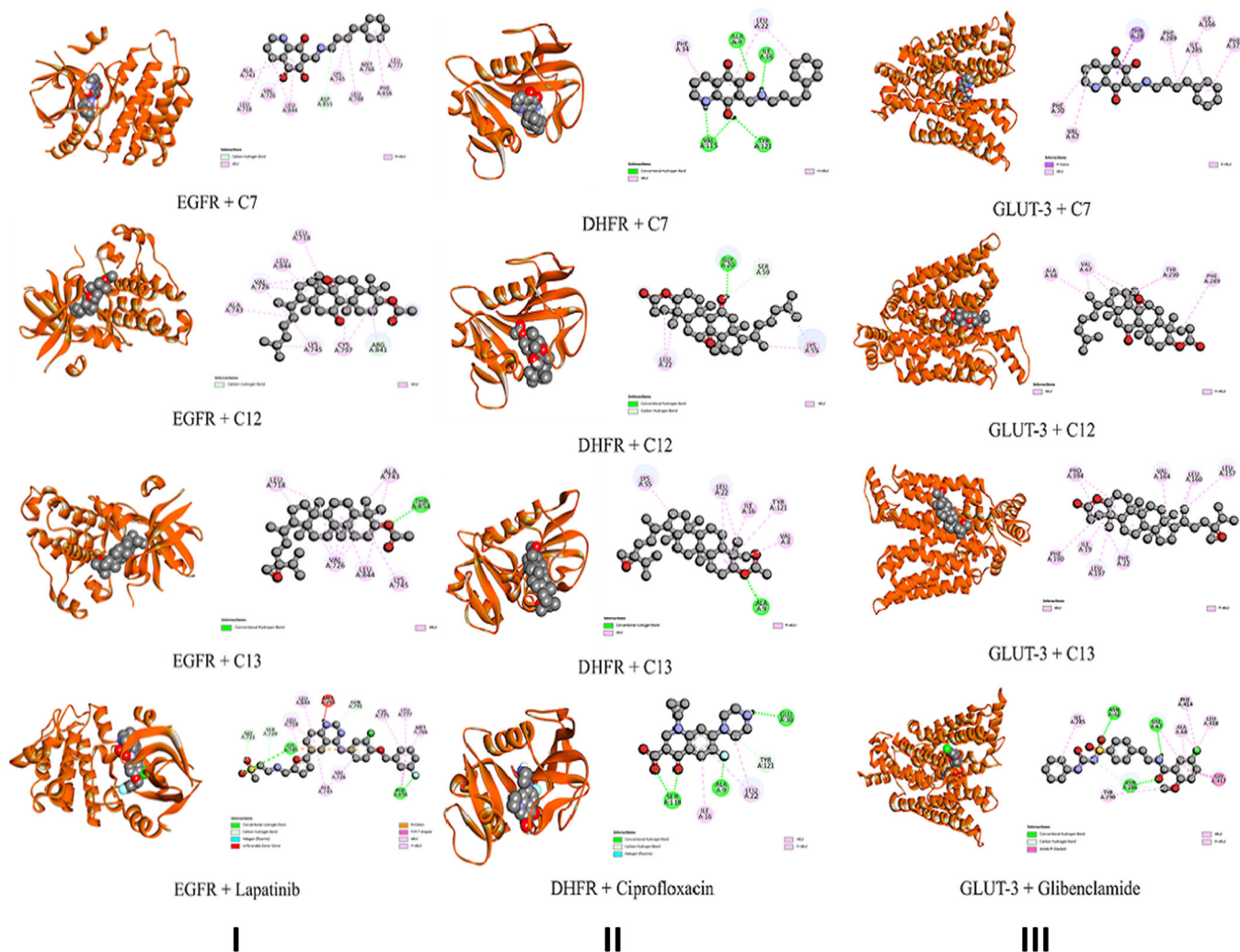
FIGURE 9 Molecular Interactions of Phytocompounds with EGFR, DHFR and GLUT-3 Enzymes: (I) Graphical representation of the molecular interactions of the most prominent phytocompounds with the EGFR enzyme in 3D visualization; (II) Graphical representation of the molecular interactions of the most prominent phytocompounds with the DHFR enzyme in 3D visualization; (III) Graphical representation of the molecular interactions of the most prominent phytocompounds with the GLUT-3 enzyme in 3D visualization.

Quinoline-5,8-dione-6-ol, 7-[[(4-cyclohexylbutyl)amino]methyl]-, in which the main functional group is found to be 5,8-quinolinedione having a wide range of effects, including as antibacterial, antifungal, anticancer, and antimalarial properties. The study of structure–activity revealed that the biological action of 5,8-quinoline-dione is due to its scaffold.[61] This compound is found to be 62% similar with the mass spectrum of the reference compound. Another compound, 2-Methylpiperidine-1-thiocarboxylic acid 2-[1-[2-thiazolyl]ethylidene] hydrazide displayed 60% (Figure 8) resemblance with the mass data. In this plant, 7,8-Epoxylanostan-11-ol, 3-acetoxy is found to be 65% similar to the reference mass spectrum, which is comparatively new compounds having antibacterial properties cited by scholars.[44] The investigation revealed the existence of several substances with significant medicinal value. Previous investigations revealed that the alcoholic compound 7,8-Epoxylanostan-11-ol, 3-acetoxy, had antibacterial and anti-inflammatory properties.[62]

4.2 | *In Silico* analysis of the compounds

EGFR, a crucial regulator of cellular processes like growth and apoptosis, undergoes conformational changes upon ligand binding, such as EGF. These changes lead to tyrosine phosphorylation in the C-terminal domain, activating downstream pathways like MAPK, PI3K/AKT, and STAT3/STAT5. Consequently, apoptosis is inhibited, and cancer-related activities are promoted.[63] Our observation implies that certain identified compounds, particularly C7 and C12 (Table 5), exhibited noteworthy affinities for EGFR. Specifically, C7 forms bonds with six alkyl groups and one C-H bond, whereas C12 forms bonds with nine alkyl groups and a single C-H bond. This is in contrast to the standard lapatinib, which has seven alkyl groups, two H atoms, three C-H bonds, and one unfavorable donor bond (Table 5, Figure 9).

Within the folate pathway, the enzyme DHFR transforms dihydrofolic acid (DHF) into tetrahydrofolic acid (THF). THF is
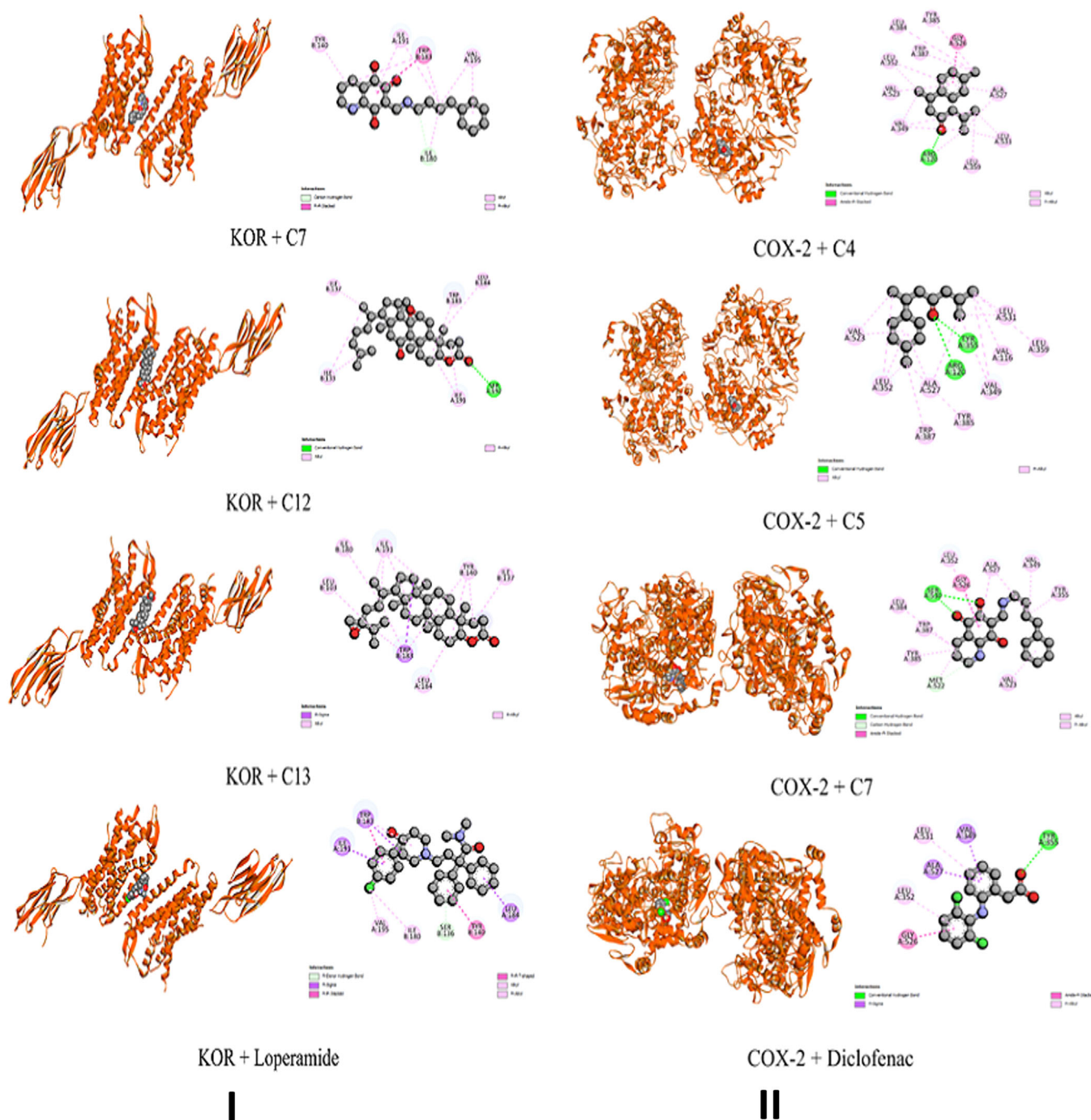
FIGURE 10 Molecular Interactions of Phytocompounds with KOR and COX-2 Enzymes: (I) Graphical representation of the molecular interactions of the most prominent phytocompounds with the KOR enzyme with 3D visualization; (II) Graphical representation of the molecular interactions of the most prominent phytocompounds with the COX-2 enzyme with 3D visualization.

essential for synthesizing amino acids and nucleic acids, critical components for cellular development and proliferation. Disruptions in the folate system lead to uncontrolled cell growth, contributing to various malignancies.[64] A couple of identified compounds exhibited activity for DHFR, suggesting their probable action against microbes. Figure 9 and Table 5 illustrate that C7 exhibited the highest −7.9 kcal/mol binding affinity by making two alkyl and four hydrogen bonds.

A specific glucose transporter protein called GLUT3 is essential to the complex mechanism of passive glucose transport through cell membranes, which is reliant on gradients in glucose concentration. Its complex role is to enable glucose molecules to migrate so they can enter or exit cells according to the relative quantities of glucose in the surrounding atmosphere. This complex regulatory mechanism is especially important in vital organs, including the kidney, pancreatic cells, and liver, where accurate

TABLE 6 ADME/T analysis result of identified compounds from methanol extract of leaves of C. assamica.

Compound No	H-bond Donor	H-bond Acceptors	Lipophilicity - log P (o/w)	GI Absorption	AMES Toxicity	Hepato-toxicity	Drug likeliness	Bioavailability score
C1	0	3	0.51	High	Yes	No	No; 1 violation: MW < 250	0.55
C2	1	3	0.53	High	No	No	No; 1 violation: MW < 250	0.55
C3	1	1	3.89	High	No	No	No; 2 violations: MW < 250, XLOGP3 > 3.5	0.55
C4	0	1	3.84	High	No	No	No; 2 violations: MW < 250, XLOGP3 > 3.5	0.55
C5	0	1	3.7	High	No	No	No; 2 violations: MW < 250, XLOGP3 > 3.5	0.55
C6	1	1	6.77	Low	No	No	No; 2 violations: Rotors > 7, XLOGP3 > 3.5	0.55
C7	2	5	3.03	High	No	Yes	No; 1 violation: XLOGP3 > 3.5	0.55
C8	1	1	5.34	High	No	No	No; 3 violations: MW < 250, Rotors > 7, XLOGP3 > 3.5	0.55
C9	1	2	2.56	High	No	Yes	Yes	0.55
C10	0	2	4.82	High	No	No	No; 2 violations: Rotors > 7, XLOGP3 > 3.5	0.55
C11	0	0	11.98	Low	No	No	No; 3 violations: MW > 350, Rotors > 7, XLOGP3 > 3.5	0.17
C12	1	4	6.61	Low	No	No	No; 2 violations: MW > 350, XLOGP3 > 3.5	0.17
C13	0	3	7.54	Low	No	No	No; 2 violations: MW > 350, XLOGP3 > 3.5	0.55
C14	0	2	7.97	Low	No	No	No; 3 violations: MW > 350, Rotors>7, XLOGP3 > 3.5	0.55
C15	1	2	3.66	High	No	No	No; 2 violations: MW > 350, XLOGP3 > 3.5	0.55

blood glucose control is necessary for the body's general physiological balance and metabolic stability.[65] It has been shown that C7 possessed the highest affinity (−9.1 kcal/mol) towards this receptor by engaging six alkyl and a single pi-sigma bond. However, the second highest affinity was observed for C13 (−8.5 kcal/mol), having eight alkyl bonds. So, probably due to the non-covalent pi-sigma interaction, C7 showed more affinity toward the receptor. Comparably, the standard glibenclamide is not only bound with six alkyl bonds but also three hydrogen bonds showing a binding affinity of −10.2 kcal/mol, suggesting elevated affinity could be the result of three hydrogen bonds (Table 5, Figure 9).

Opioid receptors in the human gastrointestinal (GI) tract, such as µ, ƙ, and δ receptors, play a significant role in regulating GI signaling. This is accomplished by blocking the enteric nerve's activity, preventing neurotransmitter release, and interfering with the excitatory and inhibitory motor pathways. As a result, these activities slow down intestinal transit, lessen enteric neuronal excitability, and alter fluid transport and secretion mechanisms. Variations in GI motility and stool consistency are the end result of these complex alterations.[66] Here, the binding affinity of C13 was satisfactory against KOR with an estimated free binding energy of −9.8 kcal/mol which suppressed loperamide score of −9.3 kcal/mol. This could be possible due to six alkyl and one pi-sigma interactions between C13 and KOR, while loperamide was found to have two alkyl, three pi-sigma, and one pi-pi and pi donor-hydrogen donor bond (Figure 10). Moreover, Table 5 represents that C7 interacted with four alkyl and one C-H bond to show a score of −8.7 kcal/mol.

Elevated COX-2 expression, induced by inflammatory stimuli, leads to the production of prostaglandins, notably PGE2. These substances are vital for generating and regulating inflammatory pain. To alleviate inflammation-related discomfort and hypersensitivity, it is crucial to inhibit COX-2.[67] The interaction between C5 and COX-2 was characterized by nine alkyl and two hydrogen bonds, resulting in a binding energy of −8.1 kcal/mol. Additionally, C7 displayed significant affinity (−8 kcal/mol) through eight alkyl bonds, one hydrogen bond, carbon-hydrogen interaction, and amide-pi bonds (Table 5, Figure 10). These interactions outperformed the diclofenac score of −7.8 kcal/mol, as diclofenac only formed three alkyl bonds, two pi-sigma bonds, and one hydrogen bond according to the standard criteria.

Additionally, Table 5 showed that surprisingly, C7 and C13 manifested very satisfactory binding scores against multiple receptors, suggesting their vast medicinal properties against multiple diseases. The ADME/T study represents these compounds' computational pharmacokinetics and toxicological profile.

Table 6 illustrates that C7 exhibits strong GI absorption and adheres to three out of Lipinski's rules, indicating favorable oral bioavailability, despite violating one rule. Additionally, it boasts a significant bioavailability score of 0.55 and demonstrates negative AMES toxicity, which means noncarcinogenic properties. However, its potential hepatotoxicity poses a challenge for future drug discovery efforts. On the contrary, C13 displays poor gastrointestinal absorption and fails to comply with half of Lipinski's rules, posing a

notable limitation for oral dosage formulations. Nonetheless, it exhibits negative AMES and hepatic toxicity, indicating a favorable safety profile. C5 and C12 breach half of Lipinski's rules, but their oral suitability differs significantly. C5, despite rule violations, exhibits high gastrointestinal absorption and a commendable bioavailability score of 0.55. In contrast, C12 displays low gastrointestinal absorption, indicating unsuitability for oral dosage forms. Notably, both compounds demonstrate safety regarding AMES and hepatic toxicity.

5 | CONCLUSION

The results imply that the compounds under study exhibit qualities that make them viable candidates for drugs targeting diverse health issues like cancer, microbial infections, diabetes, diarrhea, and pain management. Although these preliminary results are encouraging, more preclinical research, including animal testing and human subjects' clinical trials, is necessary to fully investigate the effectiveness and safety of these treatments. These additional studies are necessary to confirm the possible therapeutic uses of these substances and open the door for the creation of strong drugs for a range of illnesses.

AUTHOR CONTRIBUTIONS

Mohammad Abdullah Taher: Conceptualization; Investigation; Methodology; Formal analysis; Data curation; Writing—original draft; Validation; Software; Writing—review and editing. Ripa Kundu: Resources; Methodology. Aysha Akter Laboni: Investigation. Suriya Akter Shompa: Software. Md Moniruzzaman: Investigation. Mohammad Mahmudul Hasan: Software; Formal analysis. Hasin Hasnat: Software. Md Mehedi Hasan: Writing—review and editing. Mala Khan: Conceptualization; Supervision; Resources; Validation; Writing—review and editing.

CONFLICT OF INTEREST STATEMENT

The authors declare that they have no known competing financial interests or personal relationships that could have appeared to influence the work reported in this paper. All authors have thoroughly reviewed and endorsed the final version of the manuscript. Mohammad Abdullah Taher and Mala Khan had complete access to all study data and assumed full responsibility for data integrity and accuracy of analysis.

DATA AVAILABILITY STATEMENT

The data used in this study are available upon reasonable request from the corresponding author. Any additional information required to reproduce this work will be provided promptly.

TRANSPARENCY STATEMENT

The lead author Mohammad Abdullah Taher, Mala Khan affirms that this manuscript is an honest, accurate, and transparent account of the

study being reported; that no important aspects of the study have been omitted; and that any discrepancies from the study as planned (and, if relevant, registered) have been explained.

ORCID

Mohammad Abdullah Taher 🄳 http://orcid.org/0000-0002-0701-470X

REFERENCES

1. Srivastav VK, Egbuna C, Tiwari M. Chapter 1 - Plant secondary metabolites as lead compounds for the production of potent drugs. In: Egbuna C, et al. (Eds.) *Phytochemicals as Lead Compounds for New Drug Discovery*. Elsevier; 2020:3-14. doi:10.1016/B978-0-12-817890-4.00001-9

2. Hasan MM, Hossain MS, Taher MA, Rahman T. Evaluation of analgesic. antidiarrheal and hypoglycemic activities of wendlandia paniculata (Roxb.) DC leaves extract using mice model. *Toxicol Int*. 2021;28:155–163.

3. Hasan MM, Taher MA, Rahman MA, Muslim T. Analgesic, antidiarrheal, CNS-depressant, membrane stabilizing and cytotoxic activities of canavalia virosa (Roxb.) W&A. *Bangladesh Pharm J*. 2019;22:214–218.

4. Islam MA, Bari MS, Taher MA, Chowdhury A, Hossain MK, Rashid MA. Antidiarrheal and analgesic activities of bouea oppositifolia (Roxb.) adelb. in experimental animal model. *Bangladesh Pharm J*. 2020;23:167–171.

5. Pinkey AAH, Khan ZI, Taher MA, Soma MA. Elaeocarpus serratus l. exhibits potential analgesic and antidiarrheal activities in mice model. *Int J*. 2020;6:44–51.

6. Rahman A, Hasan MM, Taher MA, Muslim T. Analgesic, antidiarrheal and CNS-depressant activities of flemingia macrophylla (Willd.). *Bangladesh Pharm J*. 2020;23:141–145.

7. Samadd MA, Hossain MR, Taher MA, et al. Multifaceted Chemico-Pharmacological insights into *cynometra ramiflora* L.: unveiling its GC-MS, cytotoxic, thrombolytic, Anti-Inflammatory, antioxidant, Anti-Diarrheal, hypoglycemic, and analgesic potentials. *Nat Prod Commun*. 2024;19:1934578X241257377. doi:10.1177/1934578X241257377

8. Islam A, Taher MA, Soma MA, et al., 2022. Lupane triterpenoids, phytosterol, phenolic acid and fatty acid from leaves of Bouea oppositifolia (Roxb.) MEISN.

9. Mimi SS, Hasan MM, Rahman MH, Chowdhury TA. Qualitative phytochemical screening, fatty acid profile and biological studies of the bark of mallotus nudiflorus (Pitali) plant. *Toxicol Int*. 2024;31:63–72.

10. Kamil Hussain M, Saquib M, Faheem Khan M. Techniques for Extraction, Isolation, and Standardization of Bio-active Compounds from Medicinal Plants. In: Swamy MK, Akhtar MS, Eds, eds. *Natural Bio-Active Compounds: Volume 2: Chemistry, Pharmacology and Health Care Practices*. Springer; 2019:179–200. doi:10.1007/978-981-13-7205-6_8

11. Iordache A, Culea M, Gherman C, Cozar O. Characterization of some plant extracts by GC–MS. *Nucl Instrum Methods Phys Res Section B: Beam Interact Mater Atoms*. 2009;267:338–342. doi:10.1016/j.nimb.2008.10.021

12. Asiamah I, Obiri SA, Tamekloe W, Armah FA, Borquaye LS. Applications of molecular docking in natural products-based drug discovery. *Sci Afr*. 2023;20:e01593. doi:10.1016/j.sciaf.2023.e01593

13. Calixto JB. Twenty-five years of research on medicinal plants in latin america: A personal view. *J Ethnopharmacol*. 2005;100:131–134. doi:10.1016/j.jep.2005.06.004

14. Henneh I, Akrofi R, Ameyaw E, et al. Stem bark extract of sterculia setigera delile exhibits anti-inflammatory properties through membrane stabilization, inhibition of protein denaturation and prostaglandin E2 activity. *J Pharm Res Int*. 2018;22:1–11. doi:10.9734/JPRI/2018/42030

15. Oppong Bekoe E, Agyare C, Boakye YD, et al. Ethnomedicinal survey and mutagenic studies of plants used in Accra metropolis, Ghana. *J Ethnopharmacol*. 2020;248:112309. doi:10.1016/j.jep.2019.112309

16. Guerrero-Perilla C, Bernal FA, Coy-Barrera ED. Molecular docking study of naturallyoccurring compounds as inhibitors of n-myristoyl transferase towards antifungal agents discovery. *Revista Colombiana de Ciencias Químico Farmacéuticas*. 2015;44:162–178. doi:10.15446/rcciquifa.v44n2.56291

17. Pinzi L, Rastelli G. Molecular docking: shifting paradigms in drug discovery. *Int J Mol Sci*. 2019;20:4331. doi:10.3390/ijms20184331

18. Taher MA, Laboni AA, Islam MA, et al. Isolation, characterization and pharmacological potentials of methanol extract of *cassia fistula* leaves: evidenced from mice model along with molecular docking analysis. *Heliyon*. 2024;10:e28460. doi:10.1016/j.heliyon.2024.e28460

19. Fernandes G. Medicinal properties of plants from the genus cissus: a review. *J Med Plants Res*. 2012;6(16):3080–3086. doi:10.5897/JMPR11.1637

20. Dutta T, Paul A, Majumder M, Sultan RA, Emran TB. Pharmacological evidence for the use of cissus assamica as a medicinal plant in the management of pain and pyrexia. *Biochem Biophys Rep*. 2020;21:100715. doi:10.1016/j.bbrep.2019.100715

21. Xie YH, Deng P, Zhang YQ, Yu WS. Studies on the chemical constituents from Cissus assamica. *Zhong yao cai = Zhongyaocai = J Chin Med Mmater*. 2009;32:210–213.

22. Chan Y-Y, Wang C-Y, Hwang T-L, et al. The constituents of the stems of cissus assamica and their bioactivities. *Molecules*. 2018;23:2799. doi:10.3390/molecules23112799

23. Yang LC, Wang F, Liu M. A study of an endothelin antagonist from a Chinese anti-Snake venom medicinal herb. *J Cardiovasc Pharmacol*. 1998;31(suppl 1):S249–S250. doi:10.1097/00005344-199800001-00070

24. Assob JC, Kamga HL, Nsagha DS, et al. Antimicrobial and toxicological activities of five medicinal plant species from Cameroon traditional Medicine. *BMC Complement Altern Med*. 2011;11:70. doi:10.1186/1472-6882-11-70

25. Salgado JM, Mansi DN, Gagliardi A. Cissus sicyoides: analysis of glycemic control in diabetic rats through biomarkers. *J Med Food*. 2009;12:722–727. doi:10.1089/jmf.2008.0157

26. Kupchan SM, Tsou G. Tumor inhibitors. LXXXI. structure and partial synthesis of fabacein. *J Org Chem*. 1973;38:1055–1056.

27. VanWagenen BC, Larsen R, Cardellina JH, Randazzo D, Lidert ZC, Swithenbank C. Ulosantoin, a potent insecticide from the sponge *ulosa ruetzleri*. *J Org Chem*. 1993;58:335–337.

28. Kim S, Thiessen PA, Bolton EE, et al. PubChem substance and compound databases. *Nucleic Acids Res*. 2016;44:D1202–D1213.

29. Obaidullah AJ, Alanazi MM, Alsaif NA, et al. Deeper insights on cnesmone javanica blume leaves extract: chemical profiles, biological attributes, network pharmacology and molecular docking. *Plants*. 2021;10:728.

30. Duarte LJ, Bruns RE. FTIR and dispersive gas phase absolute infrared intensities of hydrocarbon fundamental bands. *Spectrochim Acta, Part A*. 2019;214:1–6. doi:10.1016/j.saa.2019.01.072

31. Kannan PP, Karthick NK, Arivazhagan G. Hydrogen bond interactions in the binary solutions of formamide with methanol: FTIR spectroscopic and theoretical studies. *Spectrochim Acta, Part A*. 2020;229:117892. doi:10.1016/j.saa.2019.117892

32. Xu J-L, Gowen AA. Time series Fourier transform infrared spectroscopy for characterization of water vapor sorption in hydrophilic and hydrophobic polymeric films. *Spectrochim Acta, Part A*. 2021;250:119371. doi:10.1016/j.saa.2020.119371

33. Chrisikou I, Orkoula M, Kontoyannis C. FT-IR/ATR solid film formation: qualitative and quantitative analysis of a Piperacillin-Tazobactam formulation. *Molecules*. 2020;25:6051. doi:10.3390/molecules25246051

34. Gorbikova E, Samsonov SA, Kalendar R. Probing the Proton-Loading site of cytochrome C oxidase using Time-Resolved Fourier transform infrared spectroscopy. *Molecules*. 2020;25:3393. doi:10.3390/molecules25153393

35. Shompa SA, Hasnat H, Riti SJ, et al. Phyto-pharmacological evaluation and characterization of the methanolic extract of the *baccaurea motleyana* müll. arg. seed: promising insights into its therapeutic uses. *Front Pharmacol*. 2024;15:1359815.

36. El Azab IH, El-Sheshtawy HS, Bakr RB, Elkanzi NAA. New 1, 2, 3-triazole-containing hybrids as antitumor candidates: design, click reaction synthesis, DFT calculations, and molecular docking study. *Molecules*. 2021;26(3):708.

37. Taher MA, Laboni AA, Shompa SA, et al. Bioactive compounds extracted from leaves of G. cyanocarpa using various solvents in chromatographic separation showed Anti-Cancer and anti-microbial potentiality in in silico approach. *Chin J Anal Chem*. 2023;51:100336. doi:10.1016/j.cjac.2023.100336

38. Khatun MCS, Muhit MA, Hossain MJ, Al-Mansur MA, Rahman SMA. Isolation of phytochemical constituents from *stevia rebaudiana* (Bert.) and evaluation of their anticancer, antimicrobial and antioxidant properties via in vitro and in silico approaches. *Heliyon*. 2021;7:e08475.

39. Mojica L, Gonzalez de Mejia E, Granados-Silvestre MÁ, Menjivar M. Evaluation of the hypoglycemic potential of a black bean hydrolyzed protein isolate and its pure peptides using in silico, in vitro and in vivo approaches. *Journal of Functional Foods*. 2017;31:274–286.

40. Alam S, Rashid MA, Sarker MMR, et al. Antidiarrheal, antimicrobial and antioxidant potentials of methanol extract of colocasia gigantea hook. f. leaves: evidenced from in vivo and in vitro studies along with computer-aided approaches. *BMC Complemen Med Ther*. 2021;21:119. doi:10.1186/s12906-021-03290-6

41. Muhammad N, Lal Shrestha R, Adhikari A, et al. First evidence of the analgesic activity of govaniadine, an alkaloid isolated from corydalis govaniana wall. *Nat Prod Res*. 2015;29:430–437.

42. Mahmud S, Rafi MO, Paul GK, et al. Designing a multi-epitope vaccine candidate to combat MERS-CoV by employing an immunoinformatics approach. *Sci Rep*. 2021;11:15431.

43. Hasnat H, Shompa SA, Richi FT, et al. Bioactive secondary metabolites to combat diabetic complications: evidenced from in silico study. *Bangladesh Pharm J*. 2023;26:167–184.

44. Alqahtani SS, Makeen HA, Menachery SJ, Moni SS. Documentation of bioactive principles of the flower from caralluma retrospiciens (Ehrenb) and in vitro antibacterial activity – part B. *Arabian J Chem*. 2020;13:7370–7377. doi:10.1016/j.arabjc.2020.07.023

45. Kumar S, Pathania AS, Nalli YK, Malik FA, Vishwakarma RA, Ali A. Synthesis of new o-alkyl and alkyne–azide cycloaddition derivatives of 4′-methoxy licoflavanone: a distinct prenylated flavonoids depicting potent cytotoxic activity. *Med Chem Res*. 2015;24:669–683. doi:10.1007/s00044-014-1177-8

46. Lu Y, Wang J, Shen G, et al. Rapid determination and quality control of pharmacological volatiles of turmeric (*Curcuma longa* L.) by fast gas Chromatography–Surface acoustic wave sensor. *Molecules*. 2021;26:5797. doi:10.3390/molecules26195797

47. Li Y-L, Du Z-Y, Li P-H, et al. Aromatic-turmerone ameliorates imiquimod-induced psoriasis-like inflammation of BALB/c mice. *Int Immunopharmacol*. 2018;64:319–325. doi:10.1016/j.intimp.2018.09.015

48. Park SY, Kim YH, Kim Y, Lee S-J. Aromatic-turmerone's anti-inflammatory effects in microglial cells are mediated by protein kinase A and heme oxygenase-1 signaling. *Neurochem Int*. 2012b;61:767–777. doi:10.1016/j.neuint.2012.06.020

49. Park SY, Jin ML, Kim YH, Kim Y, Lee SJ. Anti-inflammatory effects of aromatic-turmerone through blocking of NF-κB, JNK, and p38 MAPK signaling pathways in amyloid β-stimulated microglia. *Int Immunopharmacol*. 2012a;14:13–20. doi:10.1016/j.intimp.2012.06.003

50. Chen M, Chang YY, Huang S, et al. Aromatic-Turmerone attenuates LPS-Induced neuroinflammation and consequent memory impairment by targeting TLR4-Dependent signaling pathway. *Mol Nutr Food Res*. 2018;62:1700281. doi:10.1002/mnfr.201700281

51. Hucklenbroich J, Klein R, Neumaier B, et al. Aromatic-turmerone induces neural stem cell proliferation in vitro and in vivo. *Stem Cell Res Ther*. 2014;5:100. doi:10.1186/scrt500

52. Dohare P, Varma S, Ray M. Curcuma oil modulates the nitric oxide system response to cerebral ischemia/reperfusion injury. *Nitric oxide*. 2008b;19:1–11. doi:10.1016/j.niox.2008.04.020

53. Liju V, Jeena K, Kuttan R. An evaluation of antioxidant, anti-inflammatory, and antinociceptive activities of essential oil from *Curcuma longa*. L. *Indian J Pharmacol*. 2011;43:526–531. doi:10.4103/0253-7613.84961

54. Singh V, Jain M, Misra A, et al. Curcuma oil ameliorates insulin resistance & associated thrombotic complications in hamster & rat. *Indian J Med Res*. 2015;141:823–832. doi:10.4103/0971-5916.160719

55. Chen Z, Quan L, Zhou H, et al. Screening of active fractions from *Curcuma longa* radix isolated by HPLC and GC-MS for promotion of blood circulation and relief of pain. *J Ethnopharmacol*. 2019;234:68–75. doi:10.1016/j.jep.2018.09.035

56. Negi PS, Jayaprakasha GK, Jagan Mohan Rao L, Sakariah KK. Antibacterial activity of turmeric oil: a byproduct from curcumin manufacture. *J Agricult Food Chem*. 1999;47:4297–4300. doi:10.1021/jf990308d

57. Dohare P, Garg P, sharma U, Jagannathan N, Ray M. Neuroprotective efficacy and therapeutic window of curcuma oil: in rat embolic stroke model. *BMC Complement Altern Med*. 2008a;8:55. doi:10.1186/1472-6882-8-55

58. Liju VB, Jeena K, Kuttan R. Acute and subchronic toxicity as well as mutagenic evaluation of essential oil from turmeric (*Curcuma longa* L). *Food Chem Toxicol*. 2013;53:52–61. doi:10.1016/j.fct.2012.11.027

59. Skelin M, Rupnik M, Cencic A. Pancreatic beta cell lines and their applications in diabetes mellitus research. *ALTEX*. 2010;27:105–113. doi:10.14573/altex.2010.2.105

60. Unnikrishnan PS, Animish A, Madhumitha G, Suthindhiran K, Jayasri MA. Bioactivity guided study for the isolation and identification of antidiabetic compounds from edible Seaweed—Ulva reticulata. *Molecules*. 2022;27:8827. doi:10.3390/molecules27248827

61. Kadela-Tomanek M, Bębenek E, Chrobak E, Boryczka S. 5,8-Quinolinedione scaffold as a promising moiety of bioactive agents. *Molecules*. 2019;24:4115. doi:10.3390/molecules24224115

62. Hassan W, El-Gamal A, El-Sheddy E, Al-Oquil M, Farshori N. The chemical composition and antimicrobial activity of the essential oil of lavandula coronopifolia growing in Saudi Arabia. *J Chem Pharm Res*. 2014;6:604–615.

63. Ongko J, Setiawan JV, Feronytha AG, et al. In-silico screening of inhibitor on protein epidermal growth factor receptor (EGFR). *in: IOP Conference Series: Earth and Environmental Science*. IOP Publishing; 2022:012075.

64. Kodidela S, Pradhan SC, Muthukumaran J, Dubashi B, Santos-Silva T, Basu D. Genotype distribution of dihydrofolatereductase variants and their role in disease susceptibility to acute lymphoblastic leukemia in Indian population: an experimental and computational analysis. *J Leuk 4, 2*. 2016;4(1):1000209.

65. Simmons RA. Cell glucose transport and glucose handling during fetal and neonatal development. *in: Fetal and Neonatal Physiology*. Elsevier; 2017:428–435.

66. Pannemans J, Corsetti M. Opioid receptors in the GI tract: targets for treatment of both diarrhea and constipation in functional bowel disorders? *Curr Opin Pharmacol*. 2018;43: 53–58.

67. Camu F, Shi L, Vanlersberghe C. The role of COX-2 inhibitors in pain modulation. *Drugs*. 2003;63(suppl 1):1–7. doi:10.2165/00003495-200363001-00002